Keratin 14 Degradation and Aging in Epidermolysis Bullosa Simplex due to KLHL24 Gain-of-Function Variants

Vermeer, Mathilde C.S.C.; Silljé, Herman H.W.; Pas, Hendri H.; Andrei, Daniela; van der Meer, Peter; Bolling, Maria C.

Published in:
Journal of Investigative Dermatology

DOI:
10.1016/j.jid.2021.12.027

Publication date:
2022

AUTHOR CONTRIBUTIONS

Conceptualization: BO, SY; Data Curation: YSC, SL, SGL, BO; Formal Analysis: YSC, SL; Funding Acquisition: SY; Investigation: YSC, SL, MRR, BO, SY; Methodology: YSC, SL, BO, SY; Project Administration: MRR, KYC, BO, SY; Resources: MRR, KYC, BO, SY; Software: YSC; Supervision: BO, SY; Validation: MRR, KYC, BO, SY; Visualization: YSC, SL; Writing - Original Draft Preparation: YSC, SL; Writing - Review and Editing: YSC, SL, SGL, KYC, MRR, SY, BO

***Yu Seong Chu*[1,5], *Solam Lee*[2,5], *Sang Gyun Lee*[3], *Kee Yang Chung*[4], *Mi Ryung Roh*[3], *Sejung Yang*[1,6] and *Byungho Oh*[4,6,*]**

[1]*Department of Biomedical Engineering, Yonsei University, Wonju, Korea;* [2]*Department of Dermatology, Yonsei University Wonju College of Medicine, Wonju, Korea;* [3]*Department of Dermatology, Gangnam Severance Hospital, Cutaneous Biology Research Institute, Yonsei University College of Medicine, Seoul, Korea; and* [4]*Department of Dermatology, Severance Hospital, Cutaneous Biology Research Institute, Yonsei University College of Medicine, Seoul, Korea*

[5]*These authors contributed equally to this work.*
[6]*These authors contributed equally as senior authors.*
[*]*Corresponding author e-mail: obh505@gmail.com*

SUPPLEMENTARY MATERIAL

Supplementary material is linked to the online version of the paper at www.jidonline.org, and at https://doi.org/10.1016/j.jid.2021.012.033.

REFERENCES

Cox MAA, Cox TF. Multidimensional scaling. In Chen C, Härdle W, Unwin A. Handbook of data visualization. Berlin, Germany: Springer; 2008. p. 315–47.

Dick V, Sinz C, Mittlböck M, Kittler H, Tschandl P. Accuracy of computer-aided diagnosis of melanoma: a meta-analysis. JAMA Dermatol 2019;155:1291–9.

Han SS, Kim MS, Lim W, Park GH, Park I, Chang SE. Classification of the clinical images for benign and malignant cutaneous tumors using a deep learning algorithm. J Invest Dermatol 2018;138:1529–38.

Han SS, Park I, Eun Chang S, Lim W, Kim MS, Park GH, et al. Augmented intelligence dermatology: deep neural networks empower medical professionals in diagnosing skin cancer and predicting treatment options for 134 skin disorders. J Invest Dermatol 2020;140:1753–61.

Lee S, Chu YS, Yoo SK, Choi S, Choe SJ, Koh SB, et al. Augmented decision-making for acral lentiginous melanoma detection using deep convolutional neural networks. J Eur Acad Dermatol Venereol 2020;34:1842–50.

Mun JH, Jo G, Darmawan CC, Park J, Bae JM, Jin H, et al. Association between Breslow thickness and dermoscopic findings in acral melanoma. J Am Acad Dermatol 2018;79:831–5.

Stiegel E, Xiong D, Ya J, Funchain P, Isakov R, Gastman B, et al. Prognostic value of sentinel lymph node biopsy according to Breslow thickness for cutaneous melanoma. J Am Acad Dermatol 2018;78:942–8.

Wong SL, Faries MB, Kennedy EB, Agarwala SS, Akhurst TJ, Ariyan C, et al. Sentinel lymph node biopsy and management of regional lymph nodes in melanoma: American Society of Clinical Oncology and Society of Surgical Oncology clinical practice guideline update. J Clin Oncol 2018;36:399–413.

Keratin 14 Degradation and Aging in Epidermolysis Bullosa Simplex due to *KLHL24* Gain-of-Function Variants

Journal of Investigative Dermatology (2022) **142,** 2271–2274; doi:10.1016/j.jid.2021.12.027

TO THE EDITOR

Epidermolysis bullosa simplex is a hereditary skin blistering disorder characterized by basal intraepidermal blistering (Has et al., 2020). Pathogenic variants in several genes may underlie epidermolysis bullosa simplex. One of them is *KLHL24,* encoding KLHL24 protein. Dominantly acting *KLHL24* variants reported to be involved in epidermolysis bullosa simplex reside in the methionine start codon and result in loss of 28 *N*-terminal amino acids of the KLHL24 protein, referred to as KLHL24-ΔN28 (He et al., 2016; Lee et al., 2017; Lin et al., 2016). Although subjected to variability, the skin fragility phenotype of patients presented at birth with aplasia cutis congenita and mainly acral and pretibial skin fragility with subsequent scarring that persisted throughout early childhood and got alleviated into adolescence (Alkhalifah et al., 2018; He et al., 2016; Lee et al., 2017; Lin et al., 2016; Yenamandra et al., 2018). In the skin, ubiquitin ligase KLHL24 was shown to mediate proteasomal degradation of the basal epidermal expressed intermediate filament protein, keratin (K) 14. The more stable KLHL24-ΔN28 mutant causes excessive ubiquitination of K14 and subsequently basal keratinocyte (KC) fragility (He et al., 2016; Lin et al., 2016). Electron microscopy consistently showed a paucity of intermediate filaments in basal KCs of patients skin (He et al., 2016; Lee et al., 2017; Lin et al., 2016; Yenamandra et al., 2018), and K14 appeared fragmented in cultured KCs (He et al., 2016; Lin et al., 2016). Nonetheless, K14 fragmentation did not consistently correlate with more pronounced degrees of K14 degradation (Büchau et al., 2018) because K14 protein was unaffected (Lee et al., 2017; Yenamandra et al., 2018) or even increased (He et al., 2016) in patients. In this study, we questioned whether K14 degradation could be more profound in fetal-stage patient KCs, given the spontaneous age-related alleviation of disease severity. Previously, human induced pluripotent stem cell (hiPSC)-derived KC models have been successful in recapitulating the in vivo signature of skin disease (Ali et al., 2020; Kidwai et al., 2013). hiPSC-derived lineages exhibit

Abbreviations: hiPSC, human induced pluripotent stem cell; K, keratin; KC, keratinocyte

Accepted manuscript published online 11 January 2022; corrected proof published online 31 January 2022

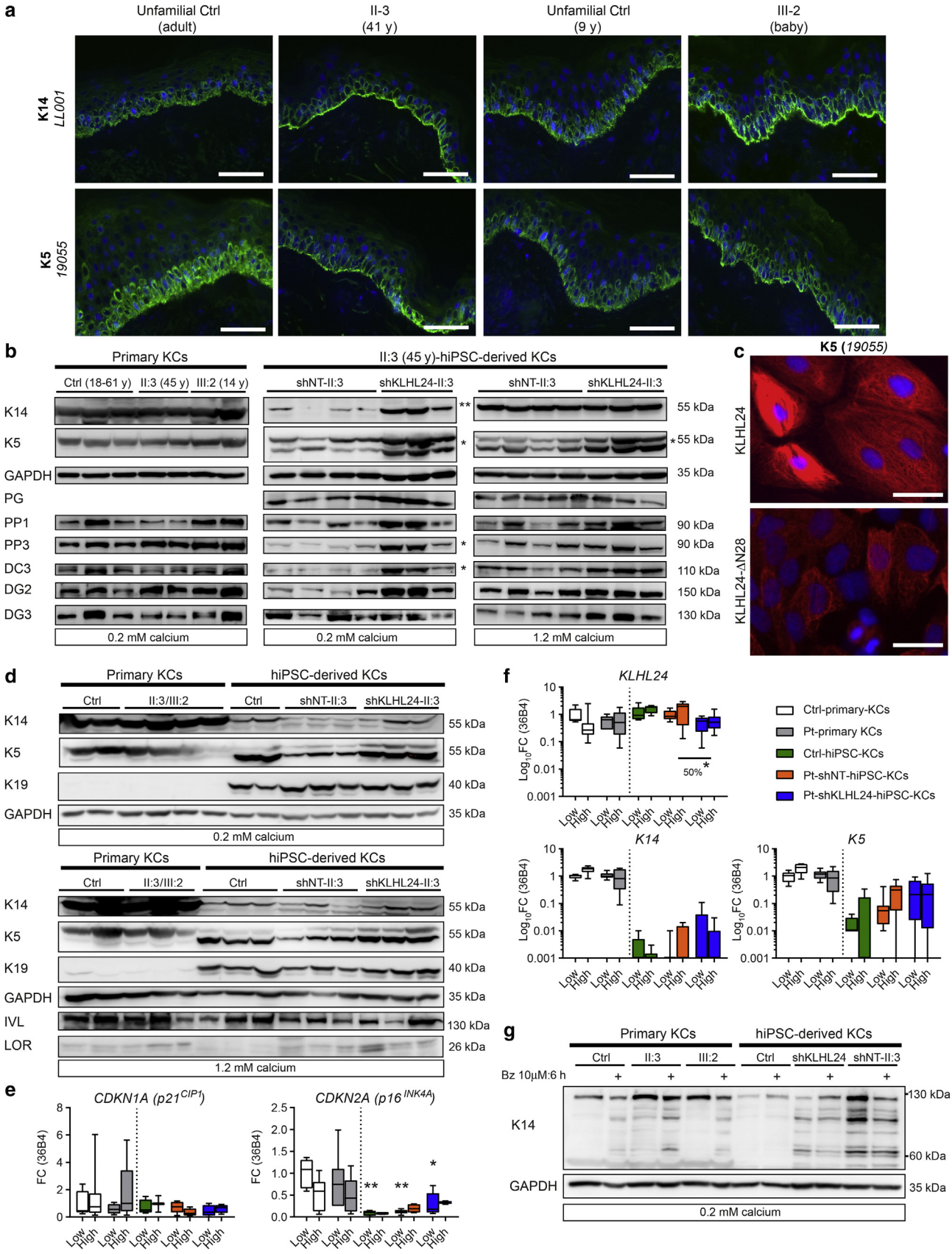

Figure 1. Comparison of primary versus hiPSC-derived KCs with a gain-of-function variant in *KLHL24*. (**a**) Immunofluorescence staining of K14 and K5 on cryosections of ex vivo skin. Bar = 200 μm. (**b**) The left panel depicts western blot analysis of K14, K5, and several desmosomal proteins (PP, DC, DG, and PG) in primary KCs from patients and nonfamilial controls. In the middle and the right panel, western blot analysis of patient II:3-hiPSC-derived KCs, with (shKLHL24) and without (shNT) RNAi of *KLHL24*, is depicted, where both undifferentiated and more differentiated KCs are derived from the same hiPSC differentiation, in

the properties of fetal-stage cells, independent of the age of the somatic cell donor (Studer et al., 2015). Furthermore, previous studies showed that RNA interference of *KLHL24* in KCs caused increased K14 protein levels (He et al., 2016; Lin et al., 2016). Therefore, by applying *KLHL24* RNA interference, we could evaluate whether K14 degradation is higher in fetal-like hiPSC-KCs than in matured primary KCs of the same individual.

Our previously reported patients (II:3 and III:2), carrying the heterozygous *KLHL24*:c.1A>G variant, had typical aplasia cutis congenita and skin fragility that improved during childhood, although dilated cardiomyopathy was diagnosed in early adulthood (Vermeer et al., 2021; Yenamandra et al., 2018). We investigated all biopsied skin samples using multiple antibodies directed against K5 and K14, which showed no marked reduction in immunofluorescence signal compared with control, albeit a slightly different distribution more at the base of basal KCs (Figure 1a and Supplementary Figure S1).

Patient-derived hiPSC with and without stable interference of *KLHL24* mRNA, previously used for engineered heart tissues to study desmin degradation (Vermeer et al., 2021), was used for KC differentiation. For both hiPSC-derived and primary KC cultures, undifferentiated KCs were maintained in CnT-PR low calcium ion conditions (CELLnTEC, Bern, Switzerland), whereas epidermal differentiation was induced using CnT-PR-D high calcium ion medium. Undifferentiated primary KCs of patients indeed showed no reduction in K5/K14 or desmosomal protein levels on quantitative western blot compared with controls (Figure 1b). In addition, vimentin expression in primary skin fibroblasts, previously affected in some other patients (He et al., 2016), was not affected and was similar to controls (Supplementary Figure S2). In contrast, the analysis indicated that K5/K14 levels were low in undifferentiated patient hiPSC-derived KCs, whereas undifferentiated hiPSC-derived KCs with RNA interference of *KLHL24* had several fold higher levels of K5 (3-fold; $P < 0.05$), K14 (4-fold; $P < 0.01$), and several desmosomal proteins (Figure 1b and c and methods described in Supplementary Figure S3). By contrast, K14 and desmosomal protein levels were steadily present after epidermal differentiation and were no longer affected by *KLHL24* knockdown in more differentiated patient hiPSC-derived KCs (Figure 1b).

To unravel differences in maturity and aging between the two culture types, we robustly investigated RNA expression and protein levels from multiple control and patient derivatives. All primary KC cultures had much higher levels of K5/K14 protein than hiPSC-derived KC cultures (Figure 1d), whereas K19, a marker of fetal but not adult KCs, was near absent in primary cultures, yet high in hiPSC-derived cultures (Tan et al., 2014). The replicate capacity (*CDKN1A*: $p21^{cip1}$) (Dabelsteen et al., 2009) of both cultures seemed similar; however, the lifespan of hiPSC-derived cultures was expected to be higher because the expression of *CDKN1B* ($p16^{INK4A}$) (Dabelsteen et al., 2009) was up to 10-fold lower ($P < 0.05$) (Figure 1e). Moreover, some keratin and desmosomal genes were differentially expressed between the two culture types (Supplementary Figure S4), which all suggests a difference in the aging and maturity status of both culture types. Although KLHL24 protein levels were too low to be detected (Supplementary Figure S5), the abundance of *KLHL24* mRNA to K14 protein was higher in hiPSC-derived than in primary KCs. Nonetheless, because this ratio did not differ between undifferentiated and more differentiated hiPSC-derived KCs (Figure 1f), the correlation of *KLHL24* to K14 is not always direct. In line with our hypothesis, ubiquitinated K14 levels were highest in patient shNT-hiPSC-derived KCs than in all other culture groups (Figure 1g and Supplementary Figure S6).

The in vivo turnover of keratins is a highly dynamic process and is critical during development and epidermal differentiation (He et al., 2016). K14 protein levels are high in basal undifferentiated layers and gradually go down toward more differentiated epidermal layers (Lin et al., 2016), whereas *KRT14* mRNA expression is only downregulated after terminal differentiation (Kopan and Fuchs, 1989). The KLHL24 ubiquitin ligase is part of the ubiquitin proteasomal system that targets K14 for proteasomal degradation. Lin et al. (2016) found the expression pattern of *KLHL24* mRNA in the skin to be opposite to the expression pattern of K14 protein. This anti-correlation was substantiated in cultured mouse KCs, where expression of *KLHL24* was higher in undifferentiated than in more differentiated KCs (Lin et al., 2016). However, we could not observe this, and our data suggest that the correlation between KLHL24 and K14 is not direct and perhaps influenced by KLHL24 (in)activity or post-translational modifications of K14 that may or may not allow targeting. Indeed, many studies with mutant KLHL24-ΔN28 cells of patients have not shown reduced K14 levels (Alkhalifah et al., 2018; He et al., 2016; Lee et al., 2017; Yenamandra et al., 2018). Contrary to their mature primary counterparts, patient hiPSC-derived

sequence from left to right. $^{**}P < 0.01$ (Mann–Whitney U test, 4-fold increase in K14 in shKLHL24 vs. shNT-KCs in low Ca^{2+}), $^{*}P < 0.05$ (3-fold increase in K5 and PP3; 2-fold increase in DG2 in shKLHL24 vs. shNT-KCs in low Ca^{2+}), and $^{*}P < 0.05$ (1.5-fold increase in K5 in shKLHL24 vs. shNT-KCs in high Ca^{2+}). (**c**) Immunofluorescence staining of K5 in Ctrl and patient hiPSC-derived KCs cultured in low Ca^{2+}. Bar = 20 μm. (**d**) Western blot analysis, corrected for equal cell counts by trypsinization, comparing primary with hiPSC-derived KCs directly (IVL, LOR, and K19) (**e**) Comparison of RNA expression specific for replication (p21) and lifespan (p16) in all culture groups. $^{*}P < 0.05$ and $^{**}P < 0.01$ (two-way ANOVA, compared with control primary KCs in low Ca^{2+}). (**f**) Comparison of RNA expression of *KLHL24*, *KRT14*, and *KRT5* in all culture groups. $^{*}P < 0.05$ (Mann–Whitney U test, *KLHL24* expression difference of 50% in shKLHL24 vs. shNT-KCs). (**g**) Western blot analysis of ubiquitinated K14 levels (>55 kDa) in undifferentiated primary versus hiPSC-derived KCs, with and without incubation with 10 μM Bz for 6 h. Functional K14 levels (55 kDa) in this blot are bleached/white due to high loading and longer exposure time. Bz, bortezomib; Ca^{2+}, calcium ion; Ctrl, control; DC, desmocollin; DG, desmoglein; FC, fold change; h, hour; hiPSC, human induced pluripotent stem cell; IVL, involucrin; K, keratin; KC, keratinocyte; LOR, loricrin; NT, not targeted; PG, plakoglobin; PP, plakophilin; Pt, patient; RNAi, RNA interference; sh, short hairpin; y, year.

KCs did show low levels of K14, suggestive of a higher degree of KLHL24-mediated degradation in these fetal-stage cells. Nonetheless, *KLHL24* knockdown only increased K14 protein levels in undifferentiated patient hiPSC-derived KCs but not in more differentiated KCs. These observations are in line with subsequent basal KC fragility in patients. In fact, keratins, other than K5/K14, become more important further up in the epidermis. Strikingly, the age-related decrease in phenotype severity is also often observed in patients with epidermolysis bullosa simplex with pathogenic *KRT5* and *KRT14* variants (Coulombe et al., 2009). In addition, K5 and K14 mutant KCs also show lower desmosomal protein levels (Liovic et al., 2009) because proper expression of K5/K14 is needed for stable desmosomal interactions (Kröger et al., 2013). Intriguingly, only in our undifferentiated patient hiPSC-derived KCs, we saw a similar trend where aberrant desmosomal protein levels normalized alongside K5/K14 after knockdown of *KLHL24*.

In conclusion, our findings indicate that K14 degradation is most pronounced in fetal-stage undifferentiated KCs of patients with start codon variants in *KLHL24*, reflecting the clinical observation of severe aplasia cutis congenita and skin fragility at birth that quickly improves over time.

Data availability statement

All data are available in the text or Supplementary Material.

ETHICS STATEMENT

The medical ethical committee of the University of Groningen (METc 2017/391; Groningen, The Netherlands) approved the participation of human subjects and all gave their written informed consent, also described in our previous publications (Vermeer et al., 2021; Yenamandra et al., 2018).

ORCIDs

Mathilde C.S.C. Vermeer: http://orcid.org/0000-0001-8513-2296
Herman H.W. Silljé: http://orcid.org/0000-0003-3292-6302
Hendri H. Pas: http://orcid.org/0000-0001-8823-2591
Daniela Andrei: http://orcid.org/0000-0003-4211-2783
Peter van der Meer: http://orcid.org/0000-0002-9705-4413
Maria C. Bolling: http://orcid.org/0000-0003-2086-9363

CONFLICT OF INTEREST

The authors state no conflict of interest.

ACKNOWLEDGMENTS

This work was supported by the Dutch Butterfly Child Foundation (grant number none, due to patient organization funding to MCB.), Human Frontier Science Program (grant number RGY 0071/2014 to PvdM), and the European Research Council (STOP-HF [StG]; grant number LS7 and ERC-2016-STG to PvdM). The authors would like to thank Albertine M. Nijenhuis for sharing her expertise in culturing keratinocytes.

AUTHOR CONTRIBUTIONS

Conceptualization: MCSCV, MCB; Data Curation: MCSCV, DA; Formal Analysis: MCSCV; Funding Acquisition: PvdM, MCB; Methodology: MCSCV, MCB; Writing - Original Draft Preparation: MCSCV; Writing - Review and Editing: MCSCV, HHWS, HHP, DA, PvdM, MCB

Mathilde C.S.C. Vermeer[1], Herman H.W. Silljé[1], Hendri H. Pas[2], Daniela Andrei[2], Peter van der Meer[1] and Maria C. Bolling[2,*]

[1]Department of Cardiology, University Medical Center Groningen, University of Groningen, Groningen, The Netherlands; and [2]Center for Blistering Diseases, Department of Dermatology, University Medical Center Groningen, University of Groningen, Groningen, The Netherlands
[*]Corresponding author e-mail: m.c.bolling@umcg.nl

SUPPLEMENTARY MATERIAL

Supplementary material is linked to the online version of the paper at www.jidonline.org, and at https://doi.org/10.1016/j.jid.2021.12.027.

REFERENCES

Ali G, Elsayed AK, Nandakumar M, Bashir M, Younis I, Abu Aqel Y, et al. Keratinocytes derived from patient-specific induced pluripotent stem cells recapitulate the genetic signature of psoriasis disease. Stem Cells Dev 2020;29:383–400.

Alkhalifah A, Chiaverini C, Charlesworth A, Has C, Lacour JP. Burnlike scars: a sign suggestive of KLHL24-related epidermolysis bullosa simplex. Pediatr Dermatol 2018;35:e193–5.

Büchau F, Munz C, Has C, Lehmann R, Magin TM. KLHL16 degrades epidermal keratins. J Invest Dermatol 2018;138:1871–3.

Coulombe PA, Kerns ML, Fuchs E. Epidermolysis bullosa simplex: a paradigm for disorders of tissue fragility. J Clin Invest 2009;119:1784–93.

Dabelsteen S, Hercule P, Barron P, Rice M, Dorsainville G, Rheinwald JG. Epithelial cells derived from human embryonic stem cells display p16INK4A senescence, hypermotility, and differentiation properties shared by many P63+ somatic cell types. Stem Cells 2009;27:1388–99.

Has C, Liu L, Bolling MC, Charlesworth AV, El Hachem M, Escámez MJ, et al. Clinical practice guidelines for laboratory diagnosis of epidermolysis bullosa. Br J Dermatol 2020;182:574–92.

He Y, Maier K, Leppert J, Hausser I, Schwieger-Briel A, Weibel L, et al. Monoallelic mutations in the translation initiation codon of KLHL24 cause skin fragility. Am J Hum Genet 2016;99:1395–404.

Kidwai FK, Liu H, Toh WS, Fu X, Jokhun DS, Movahednia MM, et al. Differentiation of human embryonic stem cells into clinically amenable keratinocytes in an autogenic environment. J Invest Dermatol 2013;133:618–28.

Kopan R, Fuchs E. A new look into an old problem: keratins as tools to investigate determination, morphogenesis, and differentiation in skin. Genes Dev 1989;3:1–15.

Kröger C, Loschke F, Schwarz N, Windoffer R, Leube RE, Magin TM. Keratins control intercellular adhesion involving PKC-α–mediated desmoplakin phosphorylation. J Cell Biol 2013;201:681–92.

Lee JYW, Liu L, Hsu CK, Aristodemou S, Ozoemena L, Ogboli M, et al. Mutations in KLHL24 add to the molecular heterogeneity of epidermolysis bullosa simplex. J Invest Dermatol 2017;137:1378–80.

Lin Z, Li S, Feng C, Yang S, Wang H, Ma D, et al. Stabilizing mutations of KLHL24 ubiquitin ligase cause loss of keratin 14 and human skin fragility. Nat Genet 2016;48:1508–16.

Liovic M, D'Alessandro M, Tomic-Canic M, Bolshakov VN, Coats SE, Lane EB. Severe keratin 5 and 14 mutations induce down-regulation of junction proteins in keratinocytes. Exp Cell Res 2009;315:2995–3003.

Studer L, Vera E, Cornacchia D. Programming and reprogramming cellular age in the era of induced pluripotency. Cell Stem Cell 2015;16:591–600.

Tan KKB, Salgado G, Connolly JE, Chan JKY, Lane EB. Characterization of fetal keratinocytes, showing enhanced stem cell-like properties: a potential source of cells for skin reconstruction. Stem Cell Reports 2014;3:324–38.

Vermeer MCSC, Bolling MC, Bliley JM, Arevalo Gomez KF, Pavez-Giani MG, Kramer D, et al. Gain-of-function mutation in ubiquitin-ligase KLHL24 causes desmin degradation and dilatation in hiPSC-derived engineered heart tissues. J Clin Invest 2021;131:e140615.

Yenamandra VK, van den Akker PC, Lemmink HH, Jan SZ, Diercks GFH, Vermeer M, et al. Cardiomyopathy in patients with epidermolysis bullosa simplex with mutations in KLHL24. Br J Dermatol 2018;179:1181–3.

SUPPLEMENTARY MATERIALS

SUPPLEMENTARY REFERENCES

Giurdanella F, Nijenhuis AM, Diercks GFH, Jonkman MF, Pas HH. Keratinocyte binding assay identifies anti-desmosomal pemphigus antibodies where other tests are negative. Front Immunol 2018;9:839.

Kidwai FK, Jokhun DS, Movahednia MM, Yeo JF, Tan KS, Cao T. Human embryonic stem cells derived keratinocyte as an in vitro research model for the study of immune response. J Oral Pathol Med 2013a;42:627–34.

Kidwai FK, Liu H, Toh WS, Fu X, Jokhun DS, Movahednia MM, et al. Differentiation of human embryonic stem cells into clinically amenable keratinocytes in an autogenic environment. J Invest Dermatol 2013b;133:618–28.

Vermeer MCSC, Bolling MC, Bliley JM, Arevalo Gomez KF, Pavez-Giani MG, Kramer D, et al. Gain-of-function mutation in ubiquitin-ligase KLHL24 causes desmin degradation and dilatation in hiPSC-derived engineered heart tissues. J Clin Invest 2021;131:e140615.

Yenamandra VK, van den Akker PC, Lemmink HH, Jan SZ, Diercks GFH, Vermeer M, et al. Cardiomyopathy in patients with epidermolysis bullosa simplex with mutations in KLHL24. Br J Dermatol 2018;179:1181–3.

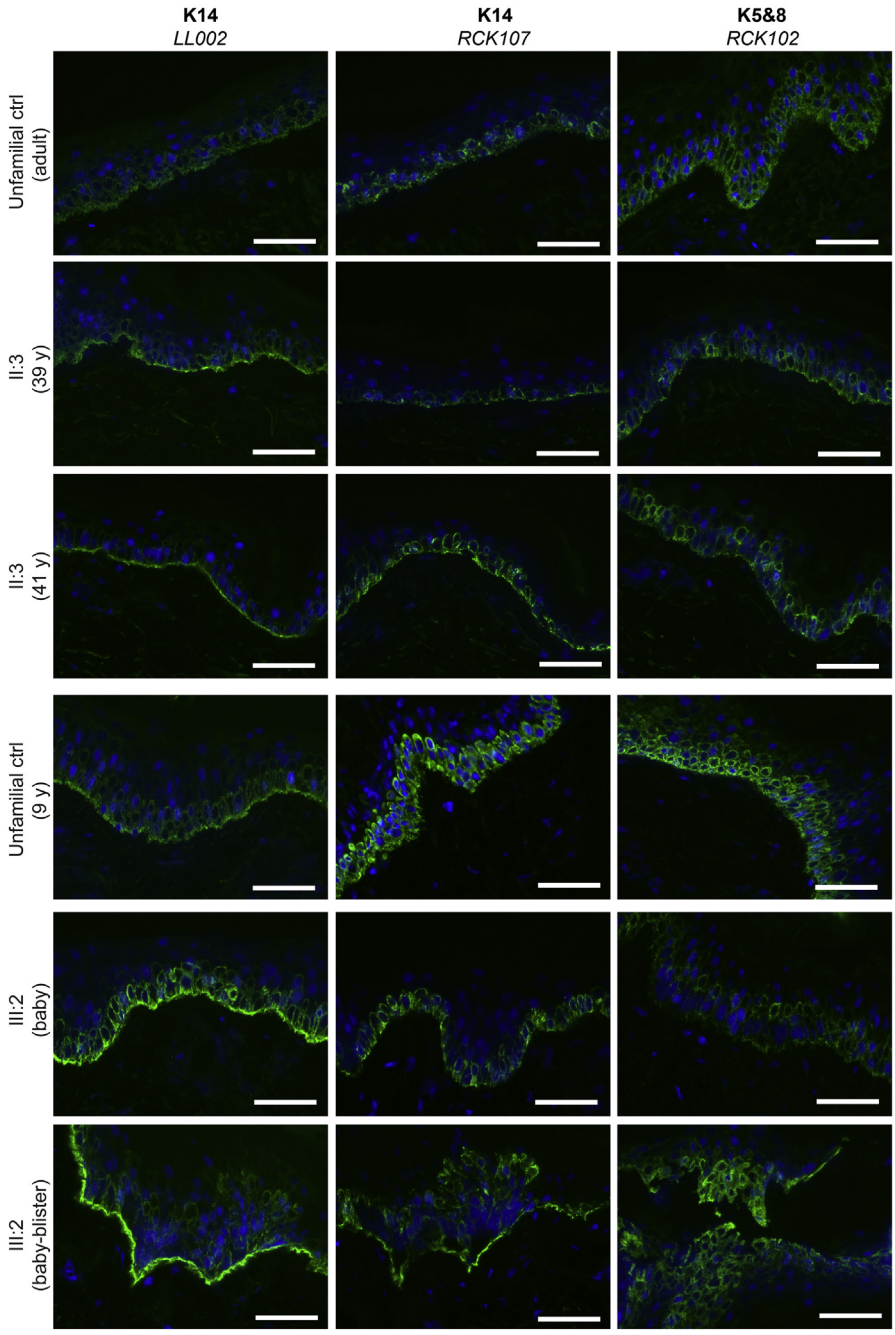

Supplementary Figure S1. Immunofluorescence staining of ex vivo skin. Immunofluorescence staining of K14 (clone LL002 and RCK107, Abcam, Cambridge, UK) and K5&8 (clone RCK102, Thermo Fisher Scientific, Waltham, MA) antigens on cryosections of all gathered patients II:3 and II:2 (KLHL24-ΔN28) skin biopsies compared with best possible age-matched nonfamilial control individuals (KLHL24). Bar = 200 μm. K, keratin; y, year.

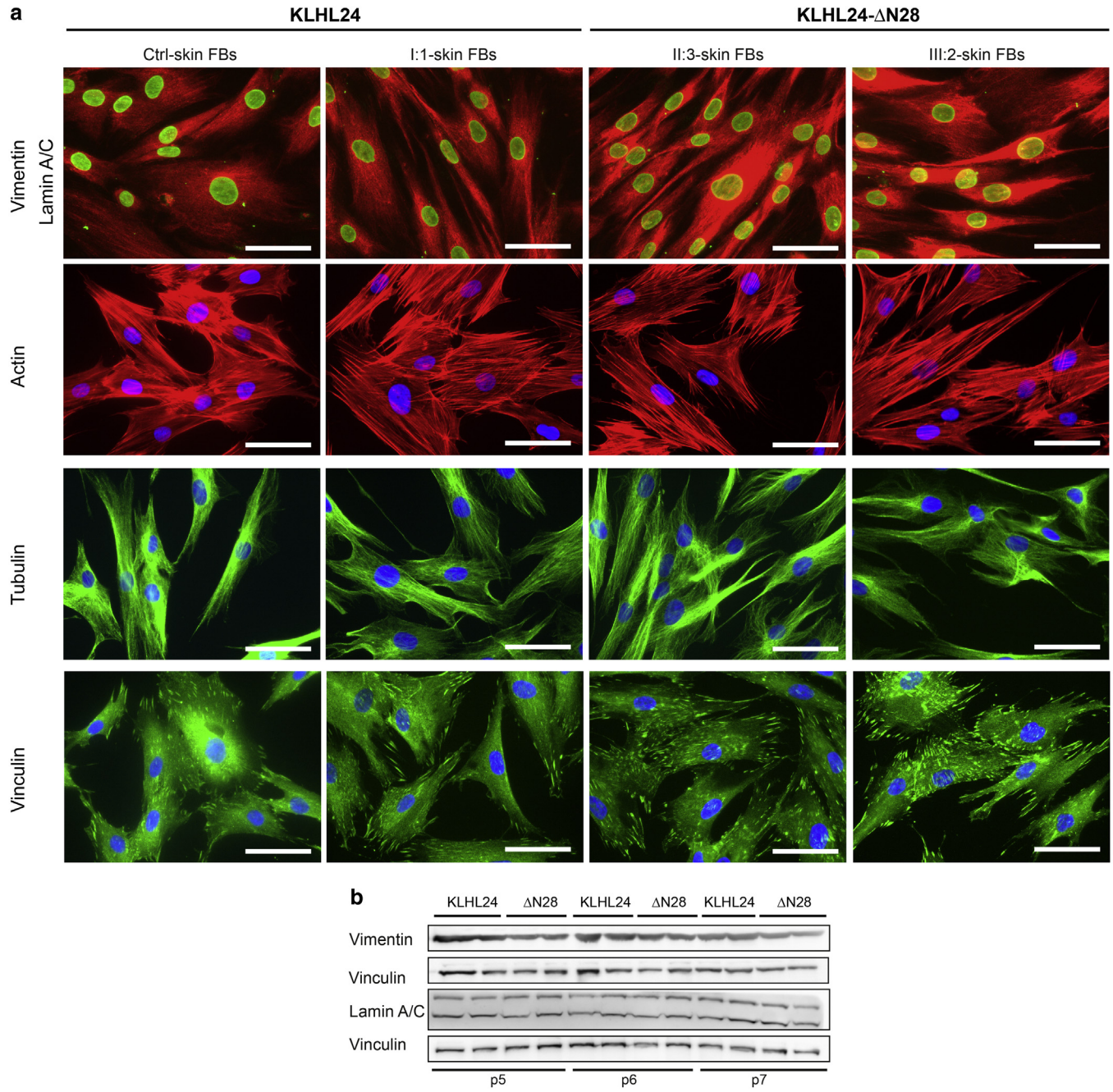

Supplementary Figure S2. Assessment of skin FBs in culture. Primary FBs, isolated from skin biopsies, were cultured in regular high glucose DMEM medium with 15% fetal calf serum and 1% P/S. (**a**) Immunofluorescence staining of vimentin (VIM 13.2, Sigma-Aldrich, St. Louis, MO), nuclear lamins (N-18, Santa Cruz Biotechnology, Santa Cruz, CA), and actin (phalloidin-rhodamine) on methanol–acetone fixated cultured skin FBs derived from biopsies of patients II:3 and II:2 (KLHL24-ΔN28) compared with one familial and one nonfamilial control individual (KLHL24). Bar = 50 μm. (**b**) Western blots showing protein levels of vimentin, lamin A and C, and vinculin in cultured skin FBs. Passage numbers are located below the blots. Ctrl, control; FB, fibroblast; P/S, penicillin/streptomycin.

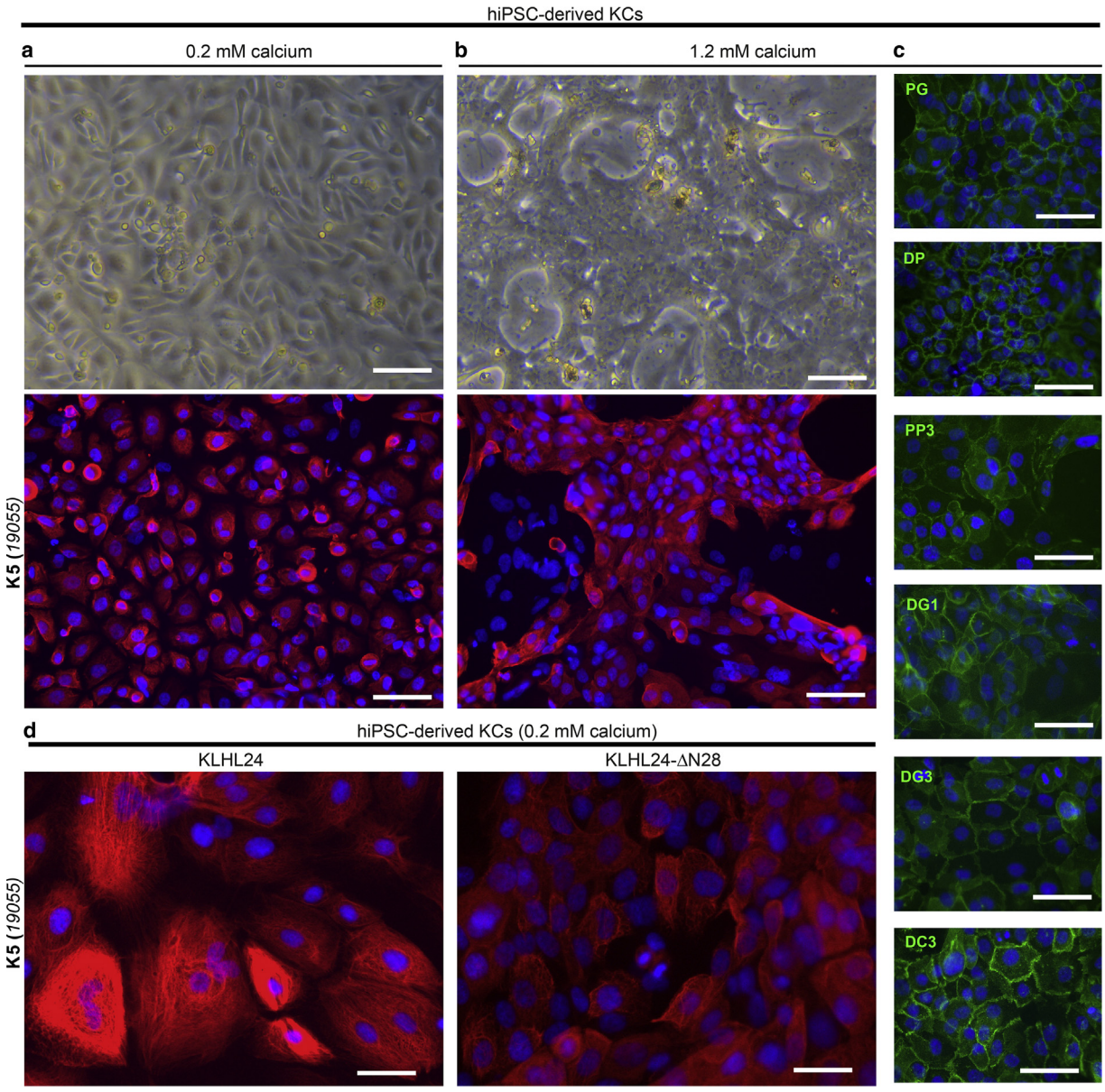

Supplementary Figure S3. Characterization of hiPSC-derived KCs. hiPSC differentiation to KCs was performed as previously described (Kidwai et al., 2013a, 2013b) with minor modifications. hiPSCs were plated on Geltrex-coated 6-well plates in E8 medium (Gibco, Thermo Fisher Scientific, Waltham, MA) using Y-27632 (Bio-Techne Corporation, Minneapolis, MN) at day −2. At day 0, hiPSCs were incubated with DMEM−HAM's F12 (3:1), 50 μg/ml ascorbic acid (Sigma-Aldrich, St. Louis, MO), 2% knockout serum replacement (Gibco, Thermo Fisher Scientific, Waltham, MA), 5 μg/ml bovine insulin solution (Sigma-Aldrich, St. Louis, MO) , 10 ng/ml hEGF (Sigma-Aldrich, St. Louis, MO), and 0.5 μM retinoic acid (Sigma-Aldrich, St. Louis, MO) until day 20 (note: high calcium medium). On days 9, 10, and 11, 25 ng/ml activin A (PeproTech, Thermo Fisher Scientific, Waltham, MA) was added to the medium. On day 20, cells were dissociated and plated on collagen-I (Corning Inc., New York, NY) and Geltrex-coated 6-well plates in CnT-PR low Ca^{2+} medium (CELLnTEC, Bern, Switzerland). Only properly differentiated KCs attached and were able to sustain the selective CnT-PR medium. With each differentiation, all cells were kept in a low Ca^{2+} medium for 4 days to proliferate until confluency. Hereinafter, half of the cells were kept as undifferentiated KCs, maintained in low Ca^{2+} conditions for another 6 days, whereas epidermal differentiation was induced in the other half of cells, using CnT-PR-D high Ca^{2+} medium for 6 days, to represent more differentiated KCs. Cells were isolated 30 days after the onset of hiPSC to KC differentiation. Primary KCs were cultured in the same media formulations from CELLnTEC as previously described (Giurdanella et al., 2018). Primary and hiPSC-derived KC cultures were free of antibiotics and regularly checked for mycoplasma contaminations. The medical ethical committee of the University of Groningen (METc 2017/391; Groningen, The Netherlands) approved the participation of human subjects and all gave their written informed consent, also described in our previous publications (Vermeer et al., 2021; Yenamandra et al., 2018). Antibodies used for western blot and/or staining are K14 (LL002, Abcam, Cambridge, UK), K5 (19055, BioLegend, San Diego, CA), DG2 (10G11, Thermo Fisher Scientific, Waltham, MA), DG3 (G194, PROGEN, Heidelberg, Germany), DC3 (U114, PROGEN, Heidelberg, Germany), DP (5A3), DG1 (EPR6766, Abcam, Cambridge, UK), PP1 (PP1-5C2, PROGEN, Heidelberg, Germany), PP3 (270.6.2, PROGEN, Heidelberg, Germany), PG (15F11, Sigma-Aldrich, St. Louis, MO), K19 (SAB2101302, Sigma-Aldrich, St. Louis, MO), IVL (Sy5, Abcam, Cambridge, UK), LOR (Poly19051, BioLegend, San Diego, CA), and loading control GAPDH (10R-G109A, Fitzgerald Industried International, Acton, MA) or vinculin (SPM227, Abcam, Cambridge, UK). (**a**) Contrast images showing the morphology of hiPSC-derived KCs in low (0.2 mM) and high (1.2 mM) calcium medium. Bar = 50 μm. (**b**) Images showing immunofluorescence K5 positive staining of 2% formalin fixated hiPSC-derived KCs in low (0.2 mM) and high (1.2 mM) calcium medium. Bar = 50 μm. (**c**) Immunofluorescence staining of hiPSC-derived KCs for desmosomal proteins after culture using high (1.2 mM) calcium medium. Bar = 50 μm. (**d**) K5 staining in hiPSC-derived KCs of control (KLHL24) and patient (KLHL24-ΔN28) in low (0.2 mM) calcium. Bar = 20 μm. A zoom-in of these images is provided in Figure 1c. Ca^{2+}, calcium ion; DC,

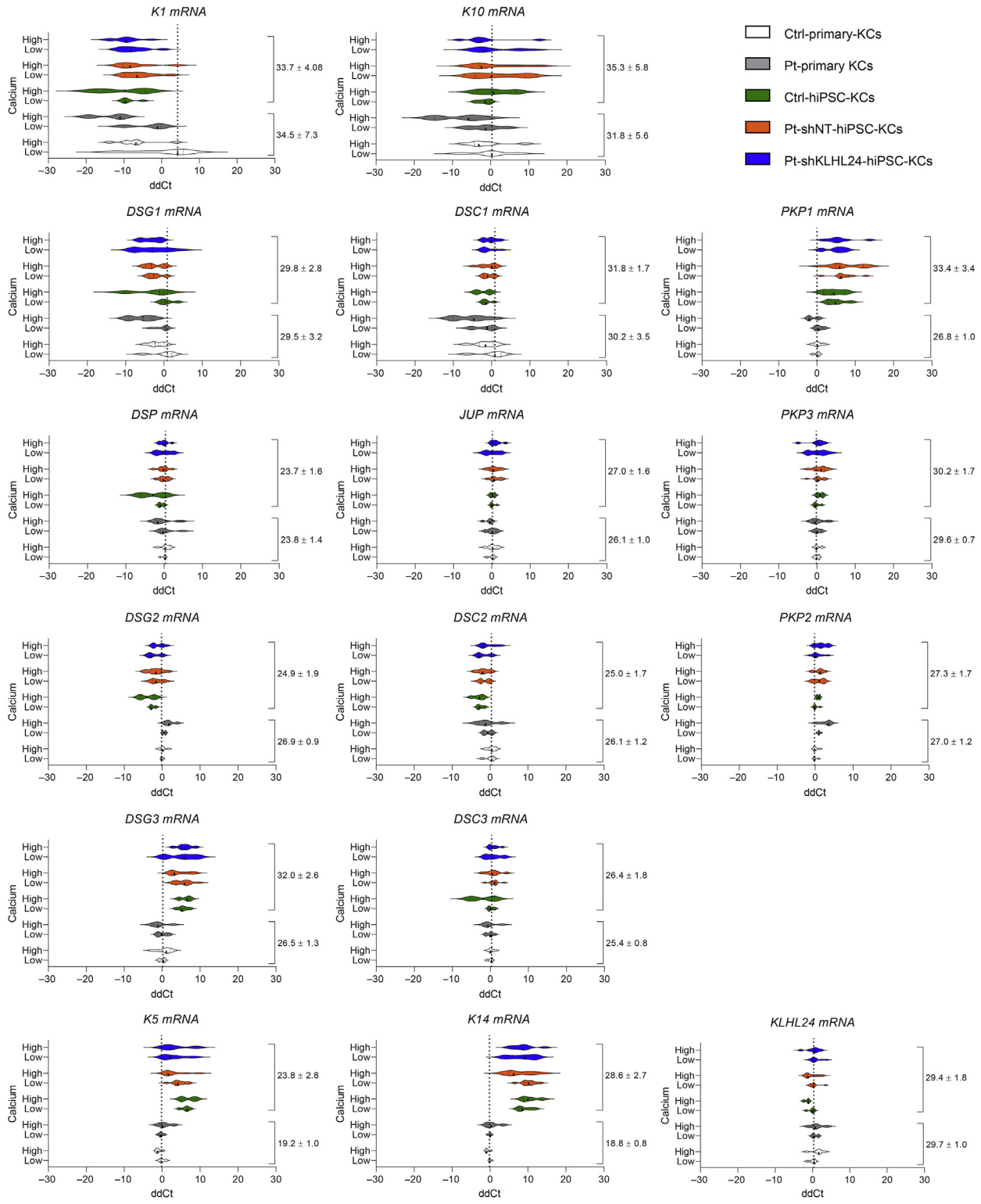

Supplementary Figure S4. Gene expression comparison of primary and hiPSC-derived KCs. Comparison of RNA expression (ddCt-values) measured in Ctrls and Pts primary KCs (passage 3−6) and Ctrls, Pt shNT, and shKLHL24-hiPSC-derived KCs cultured in 0.2 mM and 1.2 mM calcium (isolated 30 days after onset of hiPSC differentiation) using violin-plots. All groups are relative to the baseline levels of primary KCs of Ctrls cultured in 0.2 mM calcium. The negative ddCt-values represent upregulated expression levels and positive values represent downregulated expression levels. On the right side of each graph, mean ± SD of Ct-values are depicted as averages of primary KCs versus hiPSC-derived KCs. Housekeeping Ct-values for *36B4* in primary KCs are on average 19.1 ± 0.6 and in hiPSC-derived KCs 19.4 ± 0.8. Ctrl-primary-KCs (n = 5/7 samples, 4 donors), Pt-primary-KCs (n = 6/5 samples, 2 donors), Ctrl-hiPSC-derived KCs (n = 5 samples, 3 donors), Pt-shNT-hiPSC-derived KCs (n = 9 samples, 1 donor, 2 hiPSC lines), Pt-shKLHL24-hiPSC-derived KCs (n = 9 samples, 1 donor, 2 hiPSC lines). Ctrl, control; hiPSC, human induced pluripotent stem cell; KC, keratinocyte; NT, not targeted; Pt, patient; sh, short hairpin.

desmocollin; DG, desmoglein; DP, desmoplakin; hEGF, human epidermal growth factor; hiPSC, human induced pluripotent stem cell; IVL, involucrin; K, keratin; KC, keratinocyte; LOR, loricrin; PG, plakoglobin; PP plakophilin.

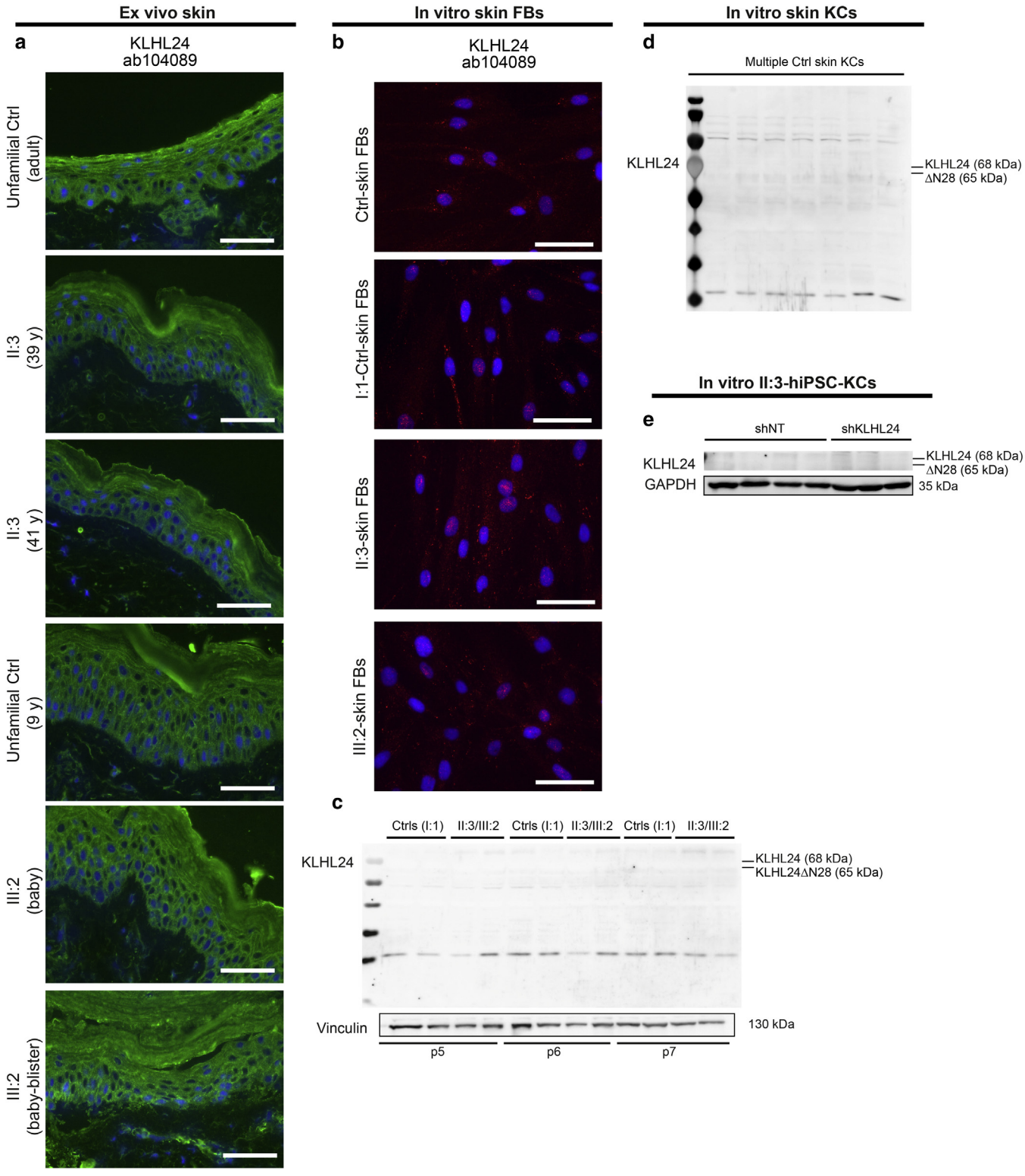

Supplementary Figure S5. Assessment of endogenous levels of KLHL24. (**a**) Visualizing immunofluorescence staining of KLHL24 (clone ab104089, Abcam, Cambridge, UK) on cryosections of all gathered patients II:3 and II:2 (KLHL24-ΔN28) skin biopsies compared with best possible age-matched nonfamilial control individuals (KLHL24). Bar = 200 μm. (**b**) Visualizing immunofluorescence staining of KLHL24 (clone ab104089) on methanol−acetone fixated cultured skin FBs derived from biopsies of patients II:3 and II:2 compared with one familial and one nonfamilial control individual. Bar = 50 μm. (**c**) Western blot showing KLHL24 protein levels in cultured skin FBs. Passage numbers are located below the blots. (**d**) Western blot showing KLHL24 protein levels in cultured skin KCs from multiple control individuals. (**e**) Western blot showing KLHL24 protein levels in patient hiPSC-derived KCs with and without RNAi of *KLHL24*. Short till long exposure times and low and higher antibody titers were used with the aim to observe KLHL24 protein levels, which remained unsuccessful. FB, fibroblast; hiPSC, human induced pluripotent stem cell; KC, keratinocyte; NT, not targeted; RNAi, RNA interference; sh, short hairpin; y, year.

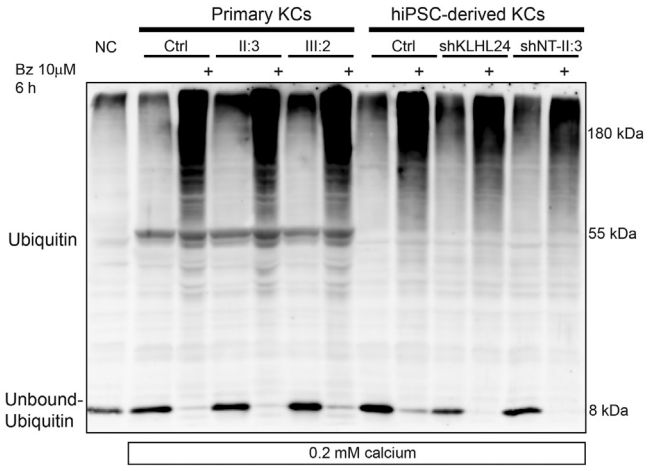

Supplementary Figure S6. Response to Bz treatment in primary and hiPSC-derived KCs. Western blot depicting broad spectrum ubiquitin antibody (FK2, Sigma-Aldrich, St. Louis, MO) detection in primary KCs and hiPSC-derived KCs, treated without and with 10 μM of Bz (Sigma-Aldrich, St. Louis, MO) for 6 h. One can observe a clear decrease in unbound-ubiquitin levels, whereas bound-ubiquitin levels increased (high kDa smear), within all the groups. Ctrl, control; h, hour; hiPSC, human induced pluripotent stem cell; Bz, bortezomib; h, hour; KC, keratinocyte; NC, negative control (derived from skin fibroblasts); NT, not targeted.